S.YU. PAVELETS, YU.N. BOBRENKO, T.V. SEMIKINA, B.S. ATDAEV,
G.I. SHEREMETOVA, M.V. YAROSHENKO

V.E. Lashkaryov Institute of Semiconductor Physics, Nat. Acad. of Sci. of Ukraine
(41, Prosp. Nauky, Kyiv 03028, Ukraine; e-mail: tanyasemikina@gmail.com)

ULTRAVIOLET SENSORS BASED ON $Zn_xCd_{1-x}S$ SOLID SOLUTIONS

Effective semiconductor ultraviolet sensors on the basis of $Zn_{0.6}Cd_{0.4}S$ and $Zn_{0.7}Cd_{0.3}$ solid solutions (SSs) are fabricated. The sensors include variband layers and a thin (~ 10 nm) stable polycrystalline $p\text{-}Cu_{1.8}S$ film as a transparent component of the surface-barrier structure. The n-CdS layers are used as substrates for the epitaxial growing of SSs. The problems of obtaining low-resistive $Zn_xCd_{1-x}S$ polycrystalline layers, providing an ohmic contact with them, and matching the lattice parameters in the SS and the substrate material are resolved by applying intermediate variband layers. On the basis of a heterostructure with glass filters, a selective sensor in the UV-A spectral interval is developed, as well as sensors sensitive to the pigmentation interval of solar radiation (the violet-blue section). Energy band diagrams of the multilayer structure are plotted. The results of Auger-spectroscopic researches and the researches of the main electrical and photovoltaic properties of sensors are reported.

K e y w o r d s: UV sensors, surface-barrier structures, solid solutions, variband layers, multilayer heterostructures, energy band diagram.

1. Introduction

The scientific direction associated with the fabrication and research of materials that are sensitive to ultraviolet (UV) radiation remains challenging for several decades. Ultraviolet sensors are required not only to be used in such traditional applied fields as medicine, biology, and ecology, but also in new ones including the UV optical communication [1], the study of the Sun and the atmosphere in the spectral interval of 300–400 nm [2], the study of the atmosphere of planets and the Martian exosphere [3], the creation of an UV nitrate sensor for mapping the ocean pollution [4], the development of an aerosol fluorescence sensor capable of detecting the biological particles in air [5], and other applications.

As a rule, UV sensors are developed on the basis of wide-energy-gap semiconductor materials [6, 7] and silicon [8]. Lately, most publications on this topic were devoted to UV sensors on the basis of zinc oxide [9, 10]. To enlarge the surface area of UV sensors for improving their parameters, zinc oxide is grown in the form of nanoparticles [11], nanowires [12–15], and nanorods [16].

Wide-energy-gap compounds A_2B_6 and their application in UV sensors have been studied for a long time, and the researches in this direction are continued [17, 18]. This interest is associated with the fact that the direct-band character of A_2B_6 compounds makes it possible to use photoactive layers of a micron-sized thickness. As a result, the thin-film design of the sensors simplifies the implementation of a planar technology for the manufacture of devices.

One of the most sensitive UV sensors was developed on the basis of the surface-barrier structure p-$Cu_{1.8}S/n$-CdS with the photosensitive component on the basis of cadmium sulfide CdS (the band gap width $E_g = 2.42$ eV) [19–21]. Their shortcoming consists in that they are sensitive in the visible spectral interval of solar radiation as well. There are sensors fabricated on the basis of the A_2B_6 compound with the maximum band gap, namely, ZnS ($E_g = 3.58$ eV). But they are not sensitive in the whole ultraviolet interval [20, 22, 23], which restricts their application scope.

The existence of a continuous series of direct-band materials (solid solutions) composed of A_2B_6 com-

pounds makes it possible to create a parametric series of photoelectric converters (PECs) with a high sensitivity in the UV spectral interval and with the long-wave edge of photoelectric effect that can be shifted from near-infrared ($\lambda = 850$ nm, if CdTe is applied) to UV ($\lambda = 360$ nm, if ZnS is applied) wavelengths. In this paper, we report about the fabrication of UV sensors on the basis of $Zn_{0.7}Cd_{0.3}S$ solid solution that are sensitive in the whole UV spectral interval and on the basis of $Zn_{0.6}Cd_{0.4}S$ solid solution that are sensitive in the pigmentation interval of solar radiation (the violet-blue section).

When growing the high-quality semiconductor layers, it is important to properly choose the substrate type. In this case, the main requirement is the isoperiodicity of the substrate and the layer which is to be grown. For example, the parameters of the GaAs and ZnSe lattices are rather close to each other, so that the application of GaAs as a substrate for depositing ZnSe made it possible the create high-quality sensors in the blue spectral interval [24, 25]. The authors of work [26] reported about the growth of the isoperiodic ZnCdS solid solution on GaP substrates. However, such an application of A_3B_5 compounds as substrates for growing layers of A_2B_6 compounds is associated with a necessity to restrict the formation of layers with a mixed composition. The formation of defect layers occurs as a result of the chemical interaction between the substrate and the vapor of elements belonging to the sixth group (S, Se) and the emergence of chalcogenide compounds A_3B_6.

In this paper, the polycrystalline CdS film is proposed to be used as a substrate for growing $Zn_xCd_{1-x}S$ solid solutions. The CdS materials possess the required properties for this purpose. In particular, there is no problem concerning the creation of ohmic contacts with CdS. Furthermore, those materials form a continuous series of SSs with materials of the grown photosensitive layers. Therefore, the problem of lattice matching between the contacting materials can be solved, by using intermediate variband layers (VLs), which is a novelty of this work. In this case, the lattice parameter changes smoothly from the substrate to the grown photoactive layer. The use of VLs excludes the possibility of the formation of undesirable chemical compounds in the transition region. In addition, photosensitive layers can be grown not only from ZnS, but from the whole continuous series of $Zn_xCd_{1-x}S$ solid solutions.

2. Sensor Fabrication

2.1. Creation of a multilayer heterostructure

The polycrystalline CdS layers 4–5 μm in thickness were grown on metallized dielectric plates, by using the quasiclosed volume method. They served as orientational substrates for the subsequent epitaxial growing of heterostructures. The concentration of major charge carriers, i.e. electrons, was determined from the measurements of the capacity-voltage characteristic following the standard procedure [27]. The corresponding value was found to lie within the interval $n = 10^{14} \div 10^{15}$ cm^{-3}.

The physical properties of CdS compounds are governed to a large extent by the concentration of intrinsic point defects of the lattice that have low ionization energies and exhibit a high electrical activity [28–30]. The control over the concentration of intrinsic defects in the lattice by changing the crystal fabrication conditions allows the concentration of free carriers in the obtained CdS specimens to be varied in a wide interval, so that a sufficiently high concentration of major charge carriers can be achieved making no additional doping with foreign impurities.

If solid solutions are applied, the situation is more complicated. Our researches showed that the application of $Zn_xCd_{1-x}S$ solid solutions with the parameter $x > 0.5$ (an elevated content of the Zn component in the SS) gives rise to technological difficulties, which do not exist for the same solid solutions, but with $x < 0.5$. Those difficulties also take place for ZnS and ZnSe [22, 31]. They consist in producing a low-ohmic SS film and creating an ohmic contact to it. In our work, this task was solved by creating a multilayer heterostructure with intermediate variband layers on the polycrystalline textured CdS substrate.

As was shown in works [22, 31], when VLs are grown on low-ohmic CdS substrates, donor-type point defects in the cadmium chalcogenide lattice stimulate the formation of corresponding defects in subsequent epitaxial layers. The intergrowth of point defects from the CdS layer through the VLs into the photoactive layer leads to the formation of $Zn_xCd_{1-x}S$ solid solution with the electron concentration $n \geq \geq 10^{16}$ cm^{-3}, which is enough for the effective operation of PECs. In addition, the formation of an intermediate VL, as was noted above, is necessary to reduce the number of structural defects associated with the lattice parameter mismatch between the photoac-
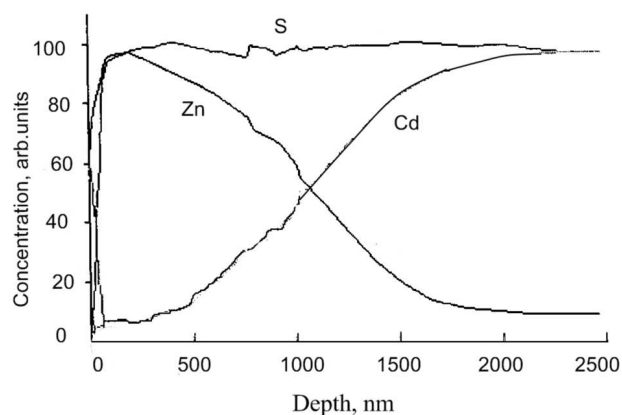
Fig. 1. Profiles of element distributions across the thickness of a ZnS/CdS heterostructure

tive epitaxial layer, $Zn_xCd_{1-x}S$, and the substrate material, CdS.

Thus, the technological process of PEC fabrication included the sequential growth of the following layers on the CdS substrate: a $Zn_xCd_{1-x}S$ variband layer with x increasing in the direction of the growth and a photosensitive layer of the $Zn_xCd_{1-x}S$ solid solution with the composition given by the parameter $x = 0.6$ or 0.7. The heterostructure was grown in a single technological cycle by the method of thermal evaporation from two independent sources of zinc and cadmium chalcogenides. The vapor was condensed on a metallized glass-ceramic substrate in a quasiclosed volume. The method used for the creation of VLs differs from the known ones [28–30, 32, 33] and allows the VLs to be obtained within the whole interval of x-values ($0 \leq x \leq 1$). In our method, the temperatures of the CdS and ZnS sources were controlled independently, which made it possible to change the component densities near the substrate and, accordingly, to govern the Zn/Cd ratio in the VL.

The parameter x in the $Zn_xCd_{1-x}S$ solid solutions was determined by measuring the band gap width E_g and the crystal lattice parameters in a particular SS. The linear dependence of E_g on the component content in the SS and the Vegard law were taken into account at that. In our experiments, the parameter x was determined to an accuracy of 3–4%. The elemental content and its variation across the thickness of condensed VL structures were studied, by using the electron Auger spectroscopy on a ultrahigh-vacuum Auger microprobe JAMP (JEOL).

The registered profiles of the elemental distribution in the ZnS/CdS system are shown in Fig. 1. One can see that the chalcogen concentration is constant across the film thickness, the zinc concentration decreases, and the cadmium one increases from the film surface to the film depth. The distributions of elements testify to a smooth transition from the SS with a Zn excess to the SS with a Cd excess in the examined materials.

2.2. Creation of the surface-barrier structure of a sensor

The basic effective structures of UV photoelectronics are the surface-barrier ones, namely, the Schottky diode [34–37] and the degenerate semiconductor-semiconductor junction [19–21]. The difficulty in creating the Schottky diodes is associated with the difficulty in producing the nano-sized metal film on the relief surface of a polycrystalline material. In this work, the degenerate semiconductor-semiconductor junction was used to create the VL. The advantage of the use of the degenerate p-$Cu_{1.8}S$ semiconductor instead of a metal in polycrystalline surface-barrier structures of VL stems from a rather high work function for p-$Cu_{1.8}S$ and a capability of growing the nano-sized (about 10 nm) $Cu_{1.8}S$ films on the relief surface of A_2B_6 polycrystalline layers.

Copper chalcogenide Cu_2S is a semiconductor with the p-type conductivity, which is determined by intrinsic defects of the vacancy type or interstitial atoms, i.e. defects induced by a deviation of the composition from the stoichiometric one. The stable phase of chalcogenides is digenite $Cu_{1.8}S$ with an electron affinity energy of 4.35 eV, a work function of 5.4–5.5 eV, a thermal forbidden band width of 0.8–0.85 eV, and the concentration of major charge carriers (holes) $p = 5 \times 10^{21}$ cm^{-3} [39, 40].

The ohmic contact was created by depositing (vacuum sputtering) a barrier-forming layer of copper sulfide with the p-type conductivity – namely, its stable modification $Cu_{1.8}S$ – onto the surface (solid solution surface) of the multilayer structure (Mo/CdS/SS). The fabricated PEC structure had inherent attributes of the surface-barrier one: owing to a drastic asymmetry between the conductivities in the contacting materials ($p = 5 \times 10^{21}$ cm^{-3} in $Cu_{1.8}S$ and $n < 10^{14}$ in the SS), the electric field was almost entirely concentrated in the base layer, i.e. the SS.

3. Energy Band Diagrams of Heterostructures and Photocurrent Spectra of Converters

Figure 2 illustrates the energy band diagrams of a multilayer heterostructure with a $Cu_{1.8}S$ barrier-forming layer. A reliable ohmic contact of the CdS layer with the metallized glass-ceramic substrate (the latter is not shown in the figure) provides the ohmic properties of the rear contact of the heterostructure. The CdS substrate of the VL provides the epitaxial growth of the photosensitive layer of the $Zn_xCd_{1-x}S$ solid solution. As one can see from Fig. 1, the elemental content of the VL deposited onto CdS smoothly changes, i.e. the transition from CdS to the photosensitive layer (the SS with a given x-value) through the VL is characterized by the absence of breaks in the c- and v-bands.

Figure 2, a exhibits a band diagram for a sensor with a photosensitive layer consisting of the $Zn_{0.7}Cd_{0.3}S$ solid solution in the case where the extension w of the space-charge region (SCR) is smaller than the SS thickness d. The band diagram in Fig. 2, b corresponds to the case where the thickness d of the photosensitive layer (SS) is smaller than w, so that the SCR extends into the VL. The energy band diagrams for heterostructures with a photosensitive layer of the $Zn_{0.6}Cd_{0.4}S$ solid solution in the case where w is smaller than the SS thickness d qualitatively correspond to those depicted in Fig. 2, a.

As one can see from the band diagrams, the barrier is much higher for holes than for electrons, and the diode dark current through the surface-barrier structure is determined by the electron component. For the studied structures, the diffusion potential U_d falls within an interval of 0.9–1.1 V, which is in agreement with the maximum values of the photoelectric force. High U_d-values are responsible for large overbarrier currents, which are shunted by tunnel currents. As a result, the recombinant-tunnel currents typical of surface-barrier structures with a transparent p-$Cu_{1.8}S$ component dominate in the sensors concerned [41, 42]. For the examined specimens with an area of 25 mm^2, the diode dark current I_0 did not exceed 10^{-12} A.

Figure 3 demonstrates the photocurrent spectra of the examined PECs. The spectra were registered on a spectrophotometer SF-26 with the help of a calibrated UV lamp. The heterostructures were illumi-
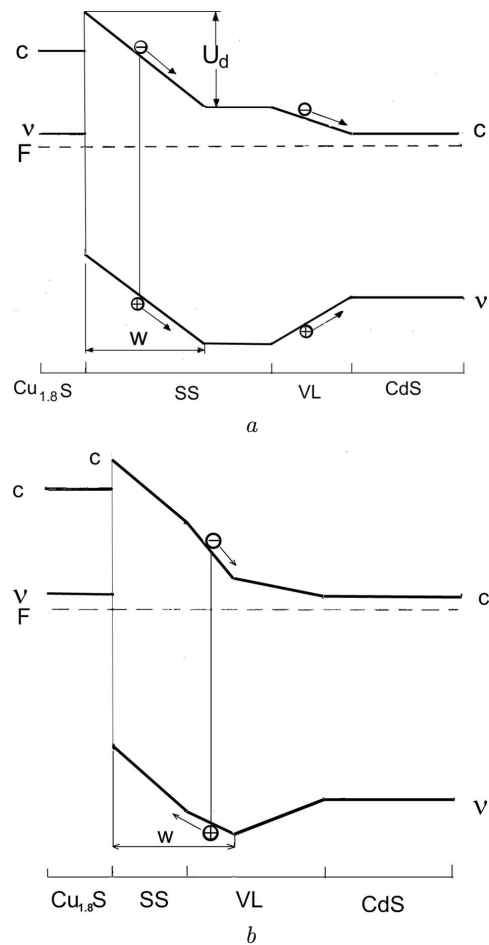
Fig. 2. Energy band diagrams for the multilayer structure of a surface-barrier photoelectric converter $Cu_{1.8}S/Zn_{0.7}Cd_{0.3}S/$ $Zn_xCd_{1-x}S$ /CdS with $d > w$ (a) and $d < w$ (b). Notations: F the Fermi level, U_d the diffusion potential, c the conduction band, v the valence band, SS the solid solution, and VL the $Zn_xCd_{1-x}S$ variband layer

nated from the $Cu_{1.8}S$ side. Curves 1 and 2 describe the photocurrent spectra for the PECs with the photosensitive layers of the $Zn_{0.6}Cd_{0.4}S$ and $Zn_{0.7}Cd_{0.3}S$ solid solutions, respectively. Curve 3 was registered for a PEC with a glass filter, which cut off the short-wave section of the spectrum for a PEC on the basis of the $Zn_{0.7}Cd_{0.3}S$ solid solution. Hence, curve 3 corresponds to the UV-A spectral interval. A PEC on the basis of the $Zn_{0.6}Cd_{0.4}$ solid solution with a glass filter (the latter is not shown in the figure) corresponds to the spectral interval where the action of the pigmentation solar radiation is maximum.
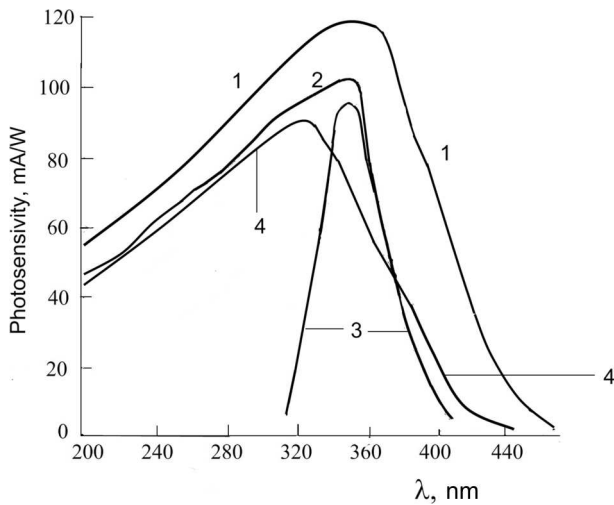
Fig. 3. Photocurrent spectra of converters: with the $Zn_{0.6}Cd_{0.4}S$ solid solution (*1*), with the $Zn_{0.7}Cd_{0.3}S$ solid solution (*2*), with the $Zn_{0.7}Cd_{0.3}S$ solid solution and a glass filter (*3*), with the $Zn_{0.7}Cd_{0.3}S$ solid solution in the case $d < w$ (*4*)

The size of photoactive region in the converters equals $w + L_d$, where L_d is the photocarrier diffusion length. In the given examples, the thickness of the SS layer $d > w + L_d$, which induces rather a drastic decrease of the photocurrent at long waves. The energy band diagram explains the absence of photoresponse. The latter is associated with the generation of charge carriers in those parts of the structure, where the energy gap is narrower in comparison with that in the SS: these are $Cu_{1.8}S$ and the transitional variband region. The potential barrier associated with the breaks in the SS and $Cu_{1.8}S$ conduction bands reduces the probability of the minor charge carrier transition from $Cu_{1.8}S$ into the SS. In addition, the electrons recombine at the defect interface $Cu_{1.8}S$–SS. The origin of photoactivity absence in the transitional VL is also evident: quasielectric fields move holes and electrons in the same direction, i.e. they do not separate the charge carriers in space.

Curve *4* in Fig. 3 illustrates the spectrum of a wrongly designed PEC. Its spectrum has no drastic long-wave recession, and its photoresponse threshold extends to $\lambda \approx 440$ nm for a PEC with the $Zn_{0.7}Cd_{0.3}S$ solid solution. This case is described by the band diagram exhibited in Fig. 2,*b*, when the SS layer thickness $d < w$, and the SCR extends into the variband layer. In this case, the extension of the photoactive region is smaller and equal to w.

4. Conclusions

On the basis of $Zn_xCd_{1-x}S$ solid solutions, selective sensors in the UV-A spectral interval (SS on the basis of $Zn_{0.7}Cd_{0.3}S$) and sensors sensitive to the pigmentation solar radiation (violet-blue spectral interval, $Zn_{0.6}Cd_{0.4}S$ solid solution) are fabricated. The sensors are found to have a rather high quantum efficiency and low diode dark currents. The original features of the sensors based on multilayer surface-barrier structures are as follows: a selected content of polycrystalline layers, the application of an ultra-thin ($\sim$10 nm) p-$Cu_{1.8}S$ film as a transparent component, and the application of intermediate variband layers. The VLs help to solve the problem of creating the low-ohmic polycrystalline layers of a $Zn_xCd_{1-x}S$ solid solution with the parameter x varying from 1 to 0.5, as well as creating ohmic contacts to them and matching the lattice parameters in the SS epitaxial layers and the substrate material. The stability of digenite $Cu_{1.8}S$ and the absence of a doping procedure with foreign impurities in the sensor fabrication technology make the sensor parameters stable. The proposed technological approach can be applied to produce structurally perfect SS layers with an arbitrary elemental content from the continuous SS series $Zn_xCd_{1-x}S$ and $Zn_xCd_{1-x}Se$.

1. J.C. Carrano, T. Li, C.J. Eiting, R.D. Dupuis, J.C. Campbell. Very high-speed ultraviolet photodetectors fabricated on GaN. *J. Electron. Mater.* **28**, 325 (1999).
2. E. Monroy, T. Palacios, O. Hainaut, F. Omnés, F. Calle, J.-F. Hochedez. Assessment of GaN metal–semiconductor–metal photodiodes for high-energy ultraviolet photodetection. *Appl. Phys. Lett.* **80**, 3198 (2002).
3. R.V.L.N. Sridhar, M.V.H. Rao, K. Kalyani, K.V.S. Bhaskar, A. Chandran, M. Mahajan, A. Bhaskar Manja, G.M. Gouda, J.D.P.V. Tayaramma, P.R. Amudha, M.M. Kandpal, K.B. Pramod, S.G. Viswanath, L.V. Prasad, A.S. Laxmiprasad, P. Chakraborty, J.A. Kamalakar, G. Nagendra Rao, M. Viswanathan. Lyman alpha photometer: a far-ultraviolet sensor for the study of hydrogen isotope ratio in the Martian exosphere. *Curr. Sci.* **109**, 1114 (2015).
4. R. Pidcock, M. Srokosz, J. Allen, M. Hartman, S. Painter, M. Mowlem, D. Hydes, A. Martin. A novel integration

of an ultraviolet nitrate sensor on board a towed vehicle for mapping open-ocean submesoscale nitrate variability. *J. Atmosph. Ocean. Technol.* **27**, 1410 (2010).

5. Jae Hee Jung, Jung Eun Lee, Gwi-Nam Bae. Real-time fluorescence measurement of airborne bacterial particles using an aerosol fluorescence sensor with dual ultraviolet- and visible-fluorescence channels. *Environm. Eng. Sci.* **29**, 987 (2012).

6. Chen Bin, Yang Yin-tang, Xie Xuan-rong, Wang Ning. Primary modeling and survey of 4H-SiC based metal–semiconductor-metal ultraviolet sensor with novel electrode structure. *Appl. Mech. Mater.* **128**–**129**, 411 (2012).

7. J. Theyirakumar, G. Gopir, B. Yatim, H. Sanusi, P.S.M. Mahmud, T.C. Hoe. Testing and calibration of an ultraviolet: A radiation sensor based on GaN photodiode. *Sains Malays.* **40**, 21 (2011).

8. Y.R. Sipauba Carvalho da Silva, Y. Koda, S. Nasuno, R. Kuroda, S. Sugawa. An ultraviolet radiation sensor using differential spectral response of silicon photodiodes. In *IEEE Sensors, Busan, South Korea, January 2015* (2015), p. 1.

9. Wang Wen-Bo, Gu Hang, He Xing-Li, Xuan Wei-Peng, Chen Jin-Kai, Wang Xiao-Zhi, Luo Ji-Kui. Transparent ZnO/glass surface acoustic wave based high performance ultraviolet light sensors. *Chin. Phys. B* **24**, 057701 (2015).

10. Jian-Wei Hoon, Kah-Yoong Chan, Zi-Neng Ng, Teck-Yong Tou. Transparent ultraviolet sensors based on magnetron sputtered ZnO thin films. *Adv. Mater. Res.* **686**, 79 (2013).

11. 11. Ki Jung Lee, Haekwan Oh, Minuk Jo, Keekeun Lee, Sang Sik Yang. An ultraviolet sensor using spin-coated ZnO nanoparticles based on surface acoustic waves. *Microelectron. Eng.* **111**, 105 (2013).

12. M.H. Mamat, N.N. Hafizah, M. Rusop, Fabrication of thin, dense and small-diameter zinc oxide nanorod array-based ultraviolet photoconductive sensors with high sensitivity by catalyst-free radio frequency magnetron sputtering. *Mater. Lett.* **93**, 215 (2013).

13. K.S. Ranjith, R.T. Rajendra Kumar, Facile construction of vertically aligned ZnO nanorod/PEDOT:PSS hybrid heterojunction-based ultraviolet light sensors: Efficient performance and mechanism. *Nanotechnology* **27**, 095304 (2016).

14. M.H. Mamat, N.D.M. Sin, I. Saurdi, N.N. Hafizah, M.F. Malek, M.N. Asiah, Z. Khusaimi, Z. Habibah, N. Nafarizal, M. Rusop. Performance of ultraviolet photoconductive sensor based on aluminium-doped zinc oxide nanorod-nanoflake network thin film using aluminium contacts. *Adv. Mater. Res.* **832**, 298 (2014).

15. M.H. Mamat, M.F. Malek, N.N. Hafizah, Z. Khusaimi, M.Z. Musa, M. Rusop, Fabrication of an ultraviolet photoconductive sensor using novel nanostructured, nanohole-enhanced, aligned aluminium-doped zinc oxide nanorod arrays at low immersion times, *Sensor. Actuat.* B **195**, 609 (2014).

16. Yung-Yu Chen, Cheng-Hsiu Ho, Tsung-Tsong Wu. Surface acoustic wave ultraviolet sensors based on ZnO nanorods. In *Proceedings of the 9th International Conference on Sensing Technology (ICST), Auckland, New Zealand* (2015), p. 406.

17. Yi Liu, Liang Xi Pang, Jing Liang, Man Kit Cheng, Jia Jun Liang, Jun Shu Chen, Ying Hoi Lai, Iam Keong Sou. A compact solid-state uv flame sensing system based on wide-gap II-VI thin film materials. *IEEE Trans. Ind. Electron.* **65** No. 3, 2737 (2018).

18. Xiaosheng Fang, Y. Bando, Meiyong Liao, Tianyou Zhai, U.K. Gautam, Liang Li, Y. Koide, D. Golberg. An efficient way to assemble ZnS nanobelts as ultraviolet-light sensors with enhanced photocurrent and stability. *Adv. Funct. Mater.* **20**, 500 (2010).

19. Yu.N. Bobrenko, A.M. Pavelets, S.Yu. Pavelets, V.M. Tkachenko. Short-wave photosensitivity of surface-barrier structures based on degenerate semiconductor–semiconductor junctions. *Pis'ma Zh. Tekhn. Fiz.* **20**, No. 12, 9 (1994) (in Russian).

20. Yu.N. Bobrenko, S.Yu. Pavelets, A.M. Pavelets, M.P. Kiselyuk, N.V. Yaroshenko. Efficient photoelectric converters of ultraviolet radiation based on ZnS and CdS with low-resistivity surface layers. *Semiconductors* **44**, 1080 (2010).

21. S.Yu. Pavelets, Yu.N. Bobrenko, T.V. Semikina, K.B. Krulikovska, G.I. Sheremetova, B.S. Atdaev, M.V. Yaroshenko. Effective policrystaline sensor of ultraviolet radiation. *Semicond. Phys. Quant. Electron. Optoelectron.* **20**, 335 (2017).

22. Yu.N. Bobrenko, S.Yu. Pavelets, A.M. Pavelets. Effective photoelectric converters of ultraviolet radiation with graded-gap ZnS-based layers. *Semiconductors* **43**, 801 (2009).

23. Yu.N. Bobrenko, S.Yu. Pavelets, A.M. Pavelets, T.V. Semikina, N.V. Yaroshenko. Surface-barrier photoconverters with graded-gap layers in the space-charge region. *Semiconductors* **49**, 519 (2015).

24. I.V. Sedova, T.V. L'vova, V.P. Ulin, S.V. Sorokin, A.V. Ankudinov, V.L. Berkovits, S.V. Ivanov, P.S. Kop'ev. Sulfide passivating coatings on GaAs(100) surface under conditions of MBE growth of $\langle II - VI \rangle$/GaAs. *Semiconductors* **36**, 54 (2002).

25. K. Ando, H. Ishikura, Y. Fukunaga, T. Kubota, H. Maeta, T. Abe, H. Kasada. Highly efficient blue-ultraviolet photodetectors basedon II-VI wide-bandgap compound semiconductors. *Phys. Status Solidi B* **229**, 1065 (2002).

26. S.V. Averin, P.I. Kuznetsov, V.A. Zhitov, N.V. Alkeev, V.M. Kotov, L.Yu. Zakharov, N.B. Gladysheva. MPM photodiodes based on wide-gap heterostructures ZnCdS/GaP. *Zh. Tekhn. Fiz.* **82**, No. 11, 49 (2012).

27. V.A. Gurtov. *Solid State Electronics: A Tutotial* (Tekhnosfera, 2008) (in Russian) [ISBN: 978-5-94836-187-1].

28. *Physics of $A^{II}B^{VI}$ compounds*. Edited by A.N. Georgobiani, M.K. Sheikman (Nauka, 1986) (in Russian).

29. G.P. Peka, V.F. Kovalenko, A.N. Smolyar. *Variband Semiconductors* (Vyshcha Shkola, 1989) (in Russian).

30. A.G. Milnes, D.L. Feucht. *Heterojunctions and Metal-Semiconductor Junctions* (Academic Press, 1972).

31. Yu.N. Bobrenko, S.Yu. Pavelets, A.M. Pavelets, N.V. Yaroshenko. Photoelectric converters with graded-gap layers based on ZnSe. *Semiconductors* **47**, 1372 (2013).

32. O.N. Tufle, E.L. Stelzer. Growth and properties of $Hg_{1-x}Cd_xTe$ epitaxial layers. *J. Appl. Phys.* **40**, 4559 (1969).

33. S. Adachi. *Properties of Group-IV, III–V and II–VI Semiconductors* (John Wiley and Sons, 2005).

34. D. Thomas, K.A. Vijayalakshmi, K.K. Sadasivuni, A. Thomas, D. Ponnamma, J.-J. Cabibihan. A fast responsive ultraviolet sensor from mSILAR-processed Sn-ZnO. *J. Electron. Mater.* **46**, 6480 (2017).

35. Chin-Wei Lin, Kuang-Lu Huang, Kai-Wei Chang, Jan-Han Chen, Kuen-Lin Chen, Chiu-Hsien Wu. Ultraviolet photodetector and gas sensor based on amorphous In-Ga-Zn-O film. *Thin Solid Films* **618**, 73 (2016).

36. T.V. Blank, Yu.A. Gol'dberg. Semiconductor photoelectric converters for the ultraviolet region of the spectrum. *Semiconductors* **37**, 999 (2003).

37. K. Hiramatsu, A. Motogaito. GaN-based Schottky barrier photodetectors from near ultraviolet to vacuum ultraviolet (360-50 nm). *Phys. Status Solidi A* **195**, 496 (2003).

38. Li Yu-Ren, Wan Chung-Yun, Chang Chia-Tsung, Tsai Wan-Lin, Huang Yu-Chih, Wang Kuang-Yu, Yang Po-Yu, Cheng Huang-Chung. Thickness effect of NiO on the performance of ultraviolet sensors with p-NiO/n-ZnO nanowire heterojunction structure. *Vacuum* **118**, 48 (2015).

39. S.Yu. Pavelets, G.A. Fedorus. Determination of the band break in Cu_2S-CdS heterojunction. *Fiz. Tekh. Poluprovodn.* **9**, 1164 (1975) (in Russian).

40. R.V. Kantariya, S.Yu. Pavelets. Energy band diagram of p-$Cu_{2-x}S$-n-CdS heterojunctions. *Fiz. Tekh. Poluprovodn.* **12**,1214 (1978) (in Russian).

41. S.Yu. Pavelets, T.M. Svanidze, V.P. Tarasenko. Specific features of current flow through degenerate semiconductor–semiconductor heterojunctions. *Ukr. Fiz. Zh.* **18**, 581 (1983) (in Russian).

42. S.Yu. Pavelets, T.V. Svanidze, V.P. Tarasenko. Reverse current in degenerate semiconductor–semiconductor heterojunctions. *Fiz. Tekh. Poluprovodn.* **17**, 1330 (1983) (in Russian).

С.Ю. Павелець, Ю.М. Бобренко, Т.В. Семікіна,
Б.С. Атдаєв, Г.Г. Шереметова, М.В. Ярошенко

СЕНСОРИ УЛЬТРАФІОЛЕТОВОГО
ВИПРОМІНЮВАННЯ НА ОСНОВІ ТВЕРДИХ
РОЗЧИНІВ $Zn_xCd_{1-x}S$

Р е з ю м е

Використання надтонкої (∼10 нм) стабільної плівки p-$Cu_{1,8}S$ в ролі прозорої складової поверхнево-бар'єрної структури, а також варізонних шарів (ВШ) дозволило отримати ефективні напівпровідникові сенсори на основі твердих розчинів (ТР) $Zn_{0,6}Cd_{0,4}S$ та $Zn_{0,7}Cd_{0,3}S$. В ролі підкладок для епітаксійного вирощування ТР використовуються шари n-CdS. Проблема одержання низькоомних полікристалічних шарів $Zn_xCd_{1-x}S$, створення до них омічних контактів, а також узгодження ґраток ТР з матеріалом підкладки вирішується шляхом використання проміжних варізонних шарів. На основі гетероструктури з використанням скляних фільтрів отримані селективний сенсор УФ-А діапазону (ТР $Zn_{0,7}Cd_{0,3}S$), а також сенсори, чутливість яких відповідає пігментаційній області сонячного випромінювання (фіолетово-блакитна область). Побудовані енергетичні зонні діаграми багатошарової гетероструктури, приведені результати оже-спектроскопічних досліджень і досліджень основних електричних і фотоелектричних властивостей сенсорів.